Journal of Cellular Biochemistry 95:611–619 (2005)

JNK/p53 Mediated Cell Death Response in K562 Exposed to Etoposide-Ionizing Radiation Combined Treatment

Nadia Sabatini,[1] Viviana Di Giacomo,[1] Monica Rapino,[2] Rosalba Rana,[1] Francesco Giusepee,[3] and Amelia Cataldi[1,4]*

[1]Dipartimento di Biomorfologia, Università G. D' Annunzio, Chieti-Pescara, Italy
[2]Istituto per i Trapianti di Organi e l'Immunocitologia del CNR, Chieti, Italy
[3]Dipartimento di Diagnostica per Immagini e Radiologia Interventistica, Policlinico Tor Vergata, Università degli Studi di Roma, Tor Vergata, Italy
[4]Cattedra di Anatomia Umana, Facoltà di Farmacia, Università G. D' Annunzio, Chieti-Pescara, Italy

Abstract The study of the ability of chemotherapeutic agents and/or ionizing radiation (IR) to induce cell death in tumor cells is essential for setting up new and more efficient therapies against human cancer. Since drug and ionizing radiation resistance is an impediment to successful chemotherapy against cancer, we wanted to check if etoposide/ionizing radiation combined treatment could have a synergic effect to improve cell death in K562, a well-known human erythroleukemia ionizing radiation resistant cell line. In this study, we examined the role played by JNK/SAPK, p53, and mitochondrial pathways in cell death response of K562 cells to etoposide and IR treatment. Our results let us suppose that the induction of cell death, already evident in 15 Gy exposed cells, mainly in 15 Gy plus etoposide, may be mediated by JNK/SAPK pathway. Moreover, p53 is a potential substrate for JNK and may act as a JNK target for etoposide and ionizing radiation. Thus further investigation on these and other molecular mechanisms underlying the cell death response following etoposide and ionizing radiation exposure could be useful to overcome resistance mechanisms in tumor cells. J. Cell. Biochem. 95: 611–619, 2005.

Key words: JNK/SAPK; p53; K562; etoposide; ionizing radiation

Ionizing radiation gives rise to a variety of cellular lesions including both DNA and membrane damage. DNA damage activates a coordinate network of signal transduction pathways involved in cell cycle arrest, apoptosis, stress response, and DNA repair processes. Etoposide, semisynthetic glycoside of podophyllotoxin, largely used against a wide range of cancers [Watters, 1999] is an inhibitor of Topoisomerase II. Unlike phodophyllotoxin, which inhibits the assembly of microtubules, the primary mode of action of etoposide is to stabilize the covalent Topoisomerase II–DNA cleavage complex by increasing its steady state concentration. For this reason Topoisomerase II becomes a physiological toxin that causes breaks in the genome of treated cells [Burden et al., 1996]. When these breaks become permanent and present at sufficient concentration trigger a series of events that ultimately culminate in cell death by apoptosis [Sabatini et al., 2004]. Apoptosis is a major form of cell death that removes redundant, damaged, or infected cells throughout life. It is important in normal cell development, and loss of control of the apoptotic program contributes to the occurrence of many diseases, including accumulation of unwanted cells through insufficient apoptosis (i.e., cancer) and cell loss as a result of excessive apoptosis (i.e., neurodegeneration) [Bratton and Cohen, 2001a]. In recent years remarkable progresses have been made in defining the central pathways of apoptosis, since an increase in apoptotic

Grant sponsor: Progetto FIRB 2001; Grant number: cod. RBAU01EN5W-001; Grant sponsor: "Interazioni tra radiazioni ionizzanti e fattori di trascrizione della famiglia CREB/CREM".

*Correspondence to: Amelia Cataldi, Dipartimento di Biomorfologia, Università G. D' Annunzio, Via dei Vestini, 6, 66100 Chieti-Pescara, Italy. E-mail: cataldi@unich.it

Received 16 July 2004; Accepted 12 November 2004

DOI 10.1002/jcb.20392

cells may be observed after exposure of cancer cells to ionizing radiation and/or anticancer drugs. Thus enhancement of apoptosis in tumor cells is an important goal for setting up medical and radioncological tumor treatment strategies.

Multiple signal transduction SS pathways are implicated in programmed cell death occurrence following exposure to IR and other cytotoxic stress factors [Verheij et al., 1998]. One of these pathways involves activation of JNK/SAPK signaling cascade, which transduces extracellular stimuli into the nucleus. In fact, activated JNK translocates to the nucleus where regulates phosphorylation of several transcription factors, such as the Jun family proteins, ATF-2, and p53 [Davis, 2000; Vogelstein et al., 2000; Shimokawa et al., 2004]. Nuclear protein p53, transcription factor and tumor suppressor which integrates numerous signals crucial to the control of life and death of cell, depending on cell type and conditions, is a key sensor of DNA damage [Amundson et al., 1998]. p53 is activated in part by various signals that induce its dissociation from its inhibitor, MDM2. Once activated p53 binds to specific DNA sequences and initiates the transcription of many genes involved in genetic stability, cell-cycle inhibition, and apoptosis [Bratton et al., 2001b]. p53-dependent apoptosis appears to be switched on by mithocondrial release of cytochrome c, which, once released from the mitochondrion, binds to the WD-40 domain and causes an unfolding of Apaf-1 (apoptosis activating factor), which exposes the nucleotide binding sites to dATP/ATP. This causes a further conformational change in Apaf-1, allowing oligodimerization and unfolding of the CARD domains, which can recruit procaspase-9. Once recruited procaspase-9 is activated and autocatalytically cleaves itself into the p37 form, rearranging and forming an active processed caspase-9, which remains tightly bound to Apaf-1. Active caspase-9 can than recruit and process the effector caspases and initiate the caspase cascade [Cain et al., 2002]. It is also suggested that the induction of apoptosis involves activation, conformational change, and homodimerization of Bax protein in the cytosol, its translocation to the outer membrane, and formation of polyprotein permeability transition pores, which, in turn, facilitate the release of apoptogenic proteins [Conus et al., 2000; Gajkowska et al., 2000].

Poly ADP-ribose polymerase (PARP) is a highly conserved enzyme that catalyses the addition of ADP-ribose polymers from NAD^+ or a variety of protein substrates, including itself and other nuclear proteins [Cookson et al., 1999]. PARP is associated with nuclear matrix [Lamarre et al., 1988] and specifically with nucleolus in cultured cells [Kaufmann et al., 1991]. PARP is cleaved by caspase-3 during apoptosis. Such damage is known to cause proliferating cells to arrest in G_1 or G_2 phase of the cell cycle.

Since drug and ionizing radiation resistance is the major impediment to successful chemotherapy against cancer, we wanted to check if the etoposide/ionizing radiation combined treatment could have a synergic effect to improve cell death in K562, a well-known human erythroleukemia IR resistant cell line. Even though many K562 clones are p53 null, based on a mutation in exon 5 characterized by a single base insertion (cytosine) between codon 135 and 136 [Law et al., 1993], it is evident that our clone, being positive to mouse monoclonal p53 antibody (Pab 240) Santa Cruz, discloses another kind of mutation, which allows exogenous p53 expression [Kremenetskaya et al., 1997]. To this aim we have paid attention to JNK/p53 metabolic pathway, largely involved in cell death induction upon exposure to different exogenous stimuli [Wu, 2004].

MATERIALS AND METHODS

Chemicals, Cell Culture, and Treatments

K562 erythroleukemic cells were grown in suspension in HEPES-buffered RPMI 1640, supplemented with 10% FCS, glutamine, penicillin/streptomycin in a controlled atmosphere. For determining optimal etoposide concentration (Sigma-Aldrich, St. Louis, MI) cells have undergone 1 h treatment with doses ranging between 1 and 10 μM. Etoposide chosen concentration was 7 μM.

Cells have been then irradiated at room temperature by a Mevatron 74 linear accelerator (Siemens, Rotterdam, Holland) (photonic energy 10 MV) administering 1.5 and 15 Gy (dose rate 3 Gy/min). When required, etoposide was added in culture 1 h prior to irradiation. Treated cells were reseeded in fresh medium and both ionizing-radiation and/or etoposide effects on cell viability were assessed by Trypan Blue dye exclusion test up to 96 h. For Western blotting analyses, cells were recovered 1 h after

ionizing radiation exposure, while for cell cycle analysis, cells were recovered 1 and 24 h after.

Clonogenicity Assay

An appropriate number of treated cells were seeded in 8 cm dishes in 7 ml of RPMI 1640 growth medium (20% FCS, 1% penicillin/streptomycin) supplemented with agar (Sigma-Aldrich) to 0.5% final concentration. Cells were incubated at 37°C in humidified air of 5% CO_2 for colony formation for a period of 14 days. Colonies containing at least 30 cells were counted. Data presented indicate mean values and standard deviations of three different experiments.

Cell Cycle Analysis

Samples containing $2-5 \times 10^5$ cells were harvested by centrifugation at 200*g* for 10 min at 4°C, fixed in 70% cold ethanol for at least 1 h at 4°C, and treated as previously detailed [Zauli et al., 1997]. Analysis of PI fluorescence was performed with an EPICS Coulter flow cytometer with FL2 detector in a linear mode using the Expo 32 analysis software. For each sample, 10,000–20,000 events were collected. Multicycle sotfware was used for cell-cycle phases analysis. For quantitative evaluation of apoptosis, subdiploid (less than 2n) DNA content was calculated as described [Secchiero et al., 1998] and expressed as percentage of apoptotic versus non-apoptotic cells, independently of the specific cell-cycle phase.

Total Homogenates

Cells, lysed in RIPA buffer (10 μg/ml aprotinin, 10 μg/ml leupeptin, 1 μg/ml PMSF, 1 mM DTT, 1mM Na_3VO_4), passaged 10 times through 25-gauge needle, were centrifuged at 10,000*g* at 4°C. The supernatant was recovered and stored at −80°C.

Isolation of Nuclei

Cells, resuspended in 10 mM Tris-HCl pH 7.4, 10 mM NaCl, 2 mM $MgCl_2$, 0.6% Triton X-100, 1.0 mM PMSF, 1 μg/ml leupeptin and aprotinin, were incubated at room temperature for 2 min, then cooled on ice for 5 min. After five passages through a 22-gauge needle, $MgCl_2$ concentration was adjusted to 5 mM. Nuclei were obtained by centrifuging the suspension at 1,200*g* for 15 min and cytoplasmic fractions consisted of the postnuclear supernatants. Nuclei were then harvested in RIPA buffer and lysed through ten passages with 25-gauge needle. Samples were centrifuged at 10,000*g* at 4°C and the supernatant stored at −80°C.

Western Blotting Analysis

Total cell lysates and nuclear proteins were electrophoresed and transferred to nitrocellulose. After blocking in 5% non-fat milk, 10 mM Tris pH 7.5, 100 mM NaCl, 0.1% Tween-20, nitrocelluloses were probed with rabbit cleaved Caspase-9 polyclonal antibody (Alexis Biochemicals, Lausen, Switzerland), mouse Bax, Bcl-2, and p53 monoclonal antibodies (Santa Cruz Biotechnology, Santa Cruz, CA), mouse caspase-3 and p-JNK/SAPK monoclonal antibodies (Cellular Signaling, New England Biolabs, Hitchin, UK), mouse PARP monoclonal antibody (Oncogene Research Products, La Jolla, CA), and developed with specific enzyme coniugated horseradish-peroxidase (Calbiochem Darmstadt, Germany). Bands were detected by ECL detection system (Amersham Intl., Buckinghamshire, UK).

Imaging and Statistics

Densitometric values of Western blotting analysis of each protein, expressed as integrated optical intensity (IOI), were estimated in a CHEMIDOC XRS System by the QuantiOne 1-D analysis software (BIORAD, Richmond, CA). Values obtained have been normalized basing on densitometric values of internal beta actin. Data were analyzed using the two tailed, two sample *T*-test. Results were expressed as mean ± SD. Values of $P < 0.05$ were considered significant.

RESULTS

The first step of our experimental model was aimed at determining the optimal etoposide concentration to combine with the two chosen radiation doses. Thus, K562 cells have undergone a preliminary treatment with concentrations ranging between 1 and 10 μM. Cells were treated for 1 h with etoposide, reseeded in fresh medium, and 24 h later processed for Trypan Blue dye exclusion test and cell cycle analysis by flow cytometry. Figure 1 and Table I show the response disclosed by K562 cells against etoposide. Both experimental results indicate 7 μM as the optimal etoposide concentration, since there is an evident cytostatic effect (G_2/M accumulation) along with a good inhibition of cell growth

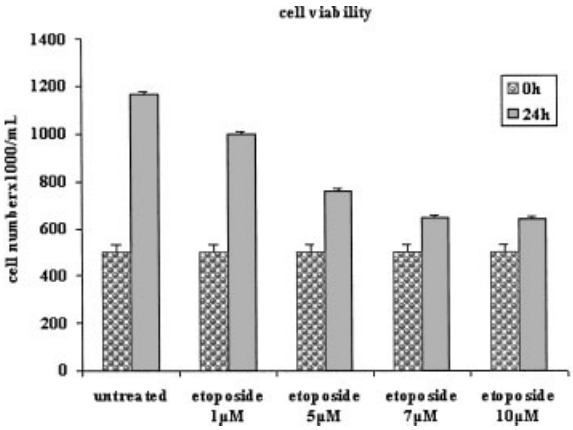

Fig. 1. Effect of different doses of etoposide on cell viability of K562 cells, determined by Trypan Blue dye exclusion test 24 h after treatment. Values are expressed as cell number ×1,000/ml ± SD.

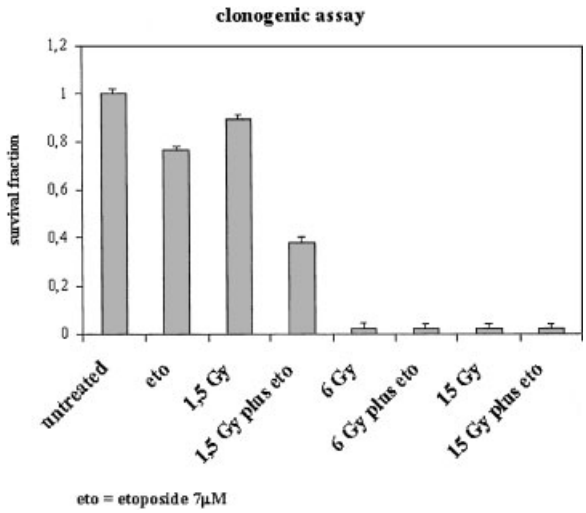

Fig. 2. The clonogenic survival of K562 cells exposed to 7 μM etoposide and/or ionizing radiation. Data presented indicate mean values and standard deviations of three different experiments, $P < 0.05$.

24 h after treatment. Concerning ionizing radiation doses administered to the cells, 1.5 Gy has been chosen as suboptimal dose, since it is the daily fraction delivered in human tumor radiotherapeutic protocols, 6 Gy intermediate one time administered dose in radiotherapy protocol, while 15 Gy has been chosen as dose useful to induce evident damage in a large number of cells and normally reached at the end of the treatment [Alridge and Ratfordi, 1998; Di Pietro et al., 2004]. Clonogenic survival assay disclosed a surviving fraction reduced to less than 50% in 1.5 Gy plus etoposide exposed sample, dramatically lowered upon 6 and 15 Gy plus or not etoposide (Fig. 2). This result is paralleled by cell cycle analysis (Table II), which shows that 48 h after IR/etoposide combined treatment there is an evident G_2/M accumulation either in 6 Gy plus etoposide or in 15 Gy plus or not etoposide samples, while the death effect is amplified after 72 and 96 h in the same experimental conditions. Thus etoposide associated to 15 Gy gives the most significant cytostatic effect. Once etoposide concentration and ionizing radiation doses have been set up, we have tried to clarify some of the molecular mechanisms underlying the occurrence of cell death upon such treatments. Since previous results by our group suggested for Jurkat T and HL60 cells a phospho-JNK/SAPK mediated apoptotic response upon etoposide/ionizing radiation combined treatment [Di Pietro et al., 2004], we wanted to check if the same metabolic pathway could be activated in K562 in the same experimental conditions. JNK activation and nuclear translocation have been associated to transcriptional events occurring early in the apoptotic process [Ham et al., 2000; Stadheim and Kucera, 2002; Willaime-Morawek et al., 2003]. Figure 3 shows nuclear translocation of phosphorylated JNK, mainly evident upon 15 and 15 Gy plus etoposide. Figure 4 shows an evident decrease of Bcl-2 expression in all treated samples mainly in 15 Gy plus etoposide, paralleled by no modification of Bax level. The decrease of Bcl-2 expression allows related Bax homodimerization, which leads to the occurrence of apoptosis, chiefly in 15 Gy plus etoposide. In addition Bax translocates to the nucleus in all treated samples except in 1.5 Gy (Fig. 4). This evidence is in accordance with recent studies demonstrating a significant Bax nuclear translocation in tumor cells stimulated to apoptosis by DNA Topoisomerase I inhibitor,

TABLE I. Evaluation of Cell Cycle by Flow-Cytometry 0 and 24 h After Exposure of K562 Erythroleukemic Cells to Different Doses of Etoposide

	h	G_1	S	G_2
Untreated	1	42.3 ± 4.0	46.4 ± 4.1	11.2 ± 1.3
Etoposide (5 μM)	1	39.2 ± 3.7	47.5 ± 5.0	13.3 ± 1.1
Etoposide (7 μM)	1	38.1 ± 4.1	49.0 ± 3.9	13.0 ± 2.0
Etoposide (10 μM)	1	42.0 ± 4.3	48.4 ± 4.2	9.6 ± 0.8
Untreated	24	37.1 ± 4.5	58.0 ± 6.0	4.9 ± 0.6
Etoposide (5 μM)	24	33.4 ± 3.6	46.3 ± 5.1	20.3 ± 1.9
Etoposide (7 μM)	24	33.0 ± 3.0	43.9 ± 4.8	23.1 ± 1.7
Etoposide (10 μM)	24	26.8 ± 2.9	44.7 ± 4.1	28.5 ± 3.1

Values are expressed as mean percentage of three different experiments ± SD.

TABLE II. Evaluation of Cell Cycle by Flow-Cytometry

	h	G_1	S	G_2	Apoptosis	Dead
Untreated	0	45.4 ± 4	45.5 ± 3	9.2 ± 0.7	2.8 ± 0.26	11.1 ± 1.2
Etopos (7 μM)	0	42.9 ± 3	47.3 ± 3.1	9.9 ± 0.7	2.6 ± 0.2	10.1 ± 0.9
1.5 Gy	0	43.9 ± 3.1	47.8 ± 4.1	8.3 ± 0.69	2.3 ± 0.21	14.1 ± 1.3
1.5 Gy + Eto (7 μM)	0	43.1 ± 3.8	46.6 ± 4.3	10.4 ± 0.9	2.1 ± 0.2	10 ± 2.1
6 Gy	0	50 ± 4.5	44.4 ± 3.6	5.6 ± 0.4	2.7 ± 0.25	22.2 ± 2.2
6 Gy + Eto 7 μM	0	43.2 ± 3.9	48.1 ± 4.1	8.7 ± 0.6	2.2 ± 0.19	10.3 ± 0.9
15 Gy	0	44.6 ± 3.1	46 ± 3.7	9.4 ± 0.8	2 ± 0.19	13.1 ± 1.1
15 Gy + Eto (7 μM)	0	43.4 ± 2.5	45.5 ± 2.1	11.1 ± 0.9	2.9 ± 0.26	10.3 ± 0.9
Untreated	24	35.9 ± 3.6	57.1 ± 3.4	7 ± 0.6	2.1 ± 0.18	11.5 ± 1.2
Etopos (7 μM)	24	24.6 ± 2.6	55.6 ± 3.6	19.8 ± 1.8	2 ± 0.17	10.1 ± 0.9
1.5 Gy	24	34.1 ± 3.2	52.6 ± 3.8	13.3 ± 1	2.2 ± 0.19	13.2 ± 1.1
1.5 Gy + Eto (7 μM)	24	24.3 ± 2	48.3 ± 4.3	27.4 ± 1.9	2.5 ± 0.2	14.4 ± 1.3
6 Gy	24	21.5 ± 1.9	40.7 ± 3.9	37.8 ± 3.1	2.7 ± 0.22	16.9 ± 1.4
6 Gy + Eto (7 μM)	24	10.3 ± 0.8	29.6 ± 2.6	60.1 ± 5.8	3.1 ± 0.27	16.2 ± 1.5
15 Gy	24	5.4 ± 5	31.4 ± 2.9	63.2 ± 6	6.4 ± 0.59	20.9 ± 1.8
15 Gy + Eto (7 μM)	24	5.4 ± 5.1	28.2 ± 2.6	66.3 ± 6.2	4.9 ± 0.4	15.4 ± 1.3
Untreated	48	31 ± 2.8	56 ± 4	12.9 ± 1.1[a]	nr	11.9 ± 0.9
Etopos (7 μM)	48	22.8 ± 2	56.2 ± 4.1	21 ± 1.9	2.5 ± 0.21	16.8 ± 1.4
1.5 Gy	48	28.2 ± 1.6	57.3 ± 4.2	14.5 ± 1.3	2.9 ± 0.23	17.1 ± 1.5
1.5 Gy + Eto (7 μM)	48	26.7 ± 2.3	55.5 ± 5.1	17.7 ± 1.5	5.2 ± 0.3	25.3 ± 2.2
6 Gy	48	24.5 ± 2.1	50.8 ± 3.5	24.7 ± 2.1	4.7 ± 0.2	31.8 ± 2.4
6 Gy + Eto (7 μM)	48	18.9 ± 1.6	43 ± 3.2	38.1 ± 3.2[a]	5.3 ± 0.7	26.4 ± 1.7
15 Gy	48	20.1 ± 1.9	18.4 ± 1.4	61.5 ± 5.8[a]	5 ± 0.4	41.1 ± 3.1
15 Gy + Eto (7 μM)	48	9.2 ± 0.7	22.3 ± 2.0	68.5 ± 6.2[a]	2.3 ± 0.2	33.6 ± 3.2
Untreated	72	42 ± 3.8	51.1 ± 5.3	6.8 ± 0.59	3.2 ± 0.4	13.8 ± 1.2[a]
Etopos (7 μM)	72	36.7 ± 3.3	54.4 ± 4.3	8.9 ± 0.7	6.5 ± 0.57	25.9 ± 1.8
1.5 Gy	72	35.2 ± 3.1	52.8 ± 3.8	12.1 ± 0.9	2.8 ± 0.19	12.7 ± 1.1
1.5 Gy + Eto (7 μM)	72	30.5 ± 3	53.7 ± 3.6	15.8 ± 1.2	8.3 ± 0.5	25 ± 1.7
6 Gy	72	21.6 ± 1.9	56 ± 3.8	22.4 ± 1.9	7.1 ± 0.61	19.7 ± 1.3
6 Gy + Eto (7 μM)	72	12.9 ± 0.8	50 ± 3.0	37.1 ± 3.2	22.4 ± 2.4	42.7 ± 2.2[a]
15 Gy	72	nr	nr	nr	nr	58 ± 3.3[a]
15 Gy + Eto (7 μM)	72	nr	nr	nr	nr	63.6 ± 4.4[a]
Untreated	96	46.2 ± 3.7	44.7 ± 3.1	9.1 ± 0.8	nr	17 ± 1.5[a]
Etopos (7 μM)	96	30.3 ± 2.6	59.9 ± 3.1	9.8 ± 0.9	6 ± 0.7	24.6 ± 2.1
1.5 Gy	96	30.5 ± 2.9	55.5 ± 3.7	14.1 ± 1.2	3.2 ± 0.23	14.4 ± 1.3
1.5 Gy + Eto (7 μM)	96	29.8 ± 2.6	48.7 ± 4.1	21.4 ± 1.8	13.2 ± 1.5	25.6 ± 1.8
6 Gy	96	24 ± 2.2	57.2 ± 4.2	18.8 ± 1.7	20.9 ± 1.9	30.5 ± 1.9
6 Gy + Eto (7 μM)	96	nr	nr	nr	nr	45 ± 3.9[a]
15 Gy	96	nr	nr	nr	nr	64.4 ± 4.5[a]
15 Gy + Eto (7 μM)	96	nr	nr	nr	nr	69 ± 5.1[a]

[a]Underlines the most significant values.

Camptothecin [Gajkowska et al., 2001]. We then wanted to clarify whether such response could be mediated by mitochondria release of cytochrome c.

In fact, many agents induce apoptosis following perturbation of mitochondria, which results in caspase activation catalyzed by a complex known as apoptosome. Once assembled the apoptosome sequentially recruits, processes, and activates caspase-9 as the initiator caspase [Saleh et al., 1999; Cain et al., 2002]. Figure 5 shows the activation of caspase-9, evidenced by 37 kDa cleaved fragment production mainly in 15 and 15 Gy plus etoposide.

The downstream effect of cleaved caspase-9 is caspase-3 activation, evidenced in Figure 6 by 20 kDa cleaved fragment production mainly in 15 and 15 Gy plus etoposide samples, confirmed, in turn, by production of PARP 85 kDa fragment into the nucleus.

Since a key sensor of DNA damage is nuclear protein p53, which in some cells appears to induce apoptosis by mitochondria-dependent-cytochrome c/Apaf-1/Caspase-9 pathway [Gao et al., 2001], we wanted to check if this important transcriptional factor could be involved along with JNK/SAPK pathway. In fact, p53 could be a potential substrate of JNK, and may act as a target in etoposide treated cells [Hu et al., 1997; Kaufmann and Earnshaw, 2000; Makin, 2002; Brantley-Finley et al., 2003].

In Figure 7, Western blotting analysis of p53 expression discloses a significant increase of protein amount, above all upon 15 Gy plus etoposide treatment.

DISCUSSION

Anticancer drugs exert in vitro and in vivo a cytostatic and apoptotic effect against tumor

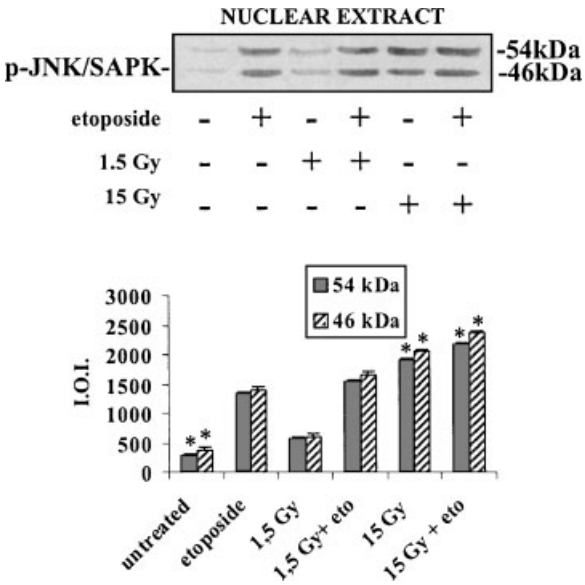

Fig. 3. Western blotting analysis of p-JNK/SAPK nuclear translocation in K562 cells exposed to 7 μM etoposide and/or ionizing radiation. Each electrophoretic lane has been loaded with equal amount of proteic lysate and protein levels have been quantified by densitometric analysis. Results are representative of three different experiments ± SD. Untreated versus 15 and 15 Gy plus etoposide, $P < 0.05$.

cells, which can imply the mitochondrial and death receptor pathways [Brantley-Finley et al., 2003].

The evidence that chemotherapy agent etoposide induces internucleosomal DNA fragmentation raised the possibility that it kills neoplastic cells through the induction of apoptosis [Wyllie et al., 1980; Lowe et al., 1994; Kamesaki et al., 1998]. In fact, etoposide, clinically useful anticancer drug, is a potent inhibitor of Topoisomerase II and DNA strand breaks, caused by the epipodophyllotoxin, when become permanent and present at sufficient concentration, lead to apoptotic death of tumor cells [Facompré et al., 2000]. However, in human hemopoietic cells DNA damage is also induced by ionizing radiation [Daniak, 2002], which determines double strand breaks and formation of more complex lesions which involve also non-DNA molecules [Schneiderman et al., 2001].

Such damages are known to cause proliferating cell to arrest in G_1 or G_2 phase of the cell cycle. These G_1 and G_2 arrest points exert a protective role against DNA damage by allowing more time for DNA repair [Leland and

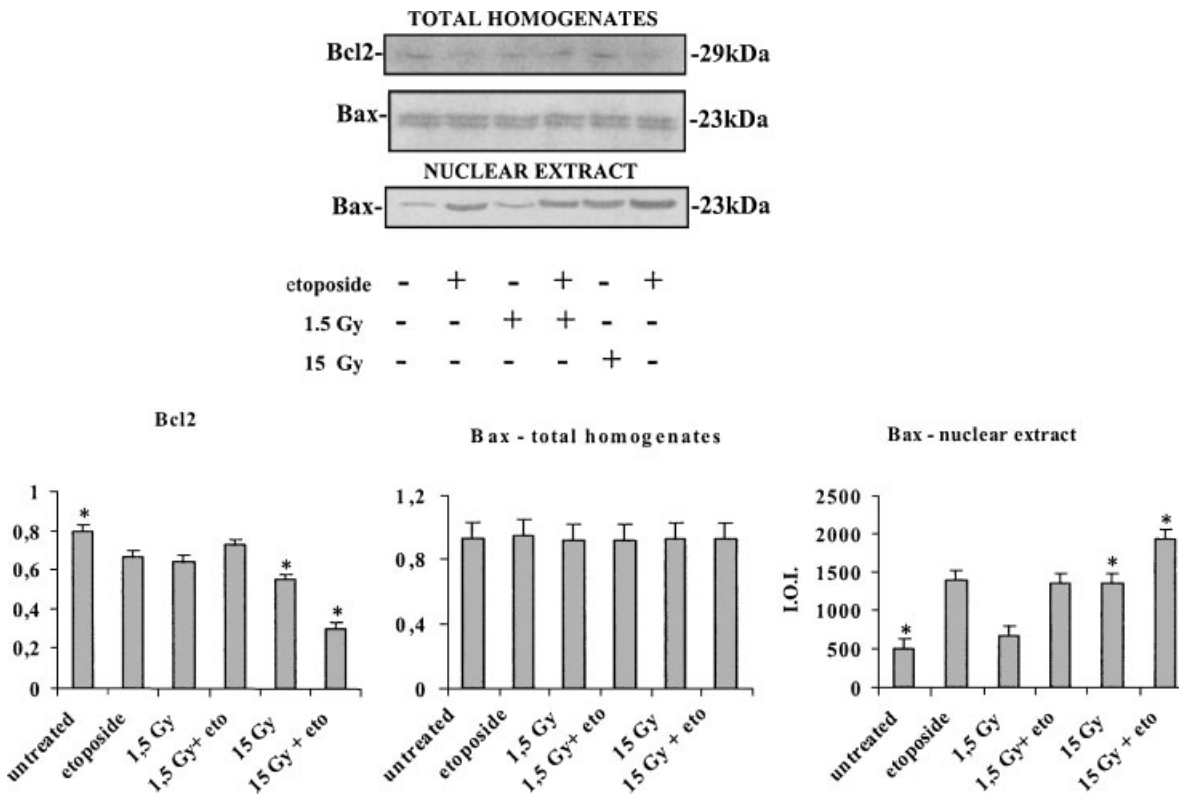

Fig. 4. Western blotting analysis of Bax and Bcl-2 expression and Bax nuclear translocation in K562 cells exposed to 7 μM etoposide and/or ionizing radiation. Each electrophoretic lane has been loaded with equal amount of proteic lysate and protein levels have been quantified by densitometric analysis. Results are representative of three different experiments ± SD. Untreated versus 15 and 15 Gy plus etoposide, $P < 0.05$.

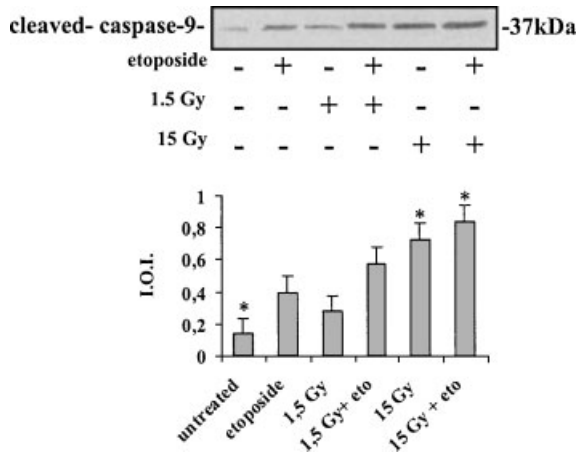

Fig. 5. Western blotting analysis of cleaved caspase-9 in K562 cells exposed to 7 μM etoposide and/or ionizing radiation. Each electrophoretic lane has been loaded with equal amount of proteic lysate and protein levels have been quantified by densitometric analysis. Results are representative of three different experiments ± SD. Untreated versus 15 and 15 Gy plus etoposide, $P < 0.05$.

Weinert, 1989; Strasser et al., 1994; Arita et al., 1997]. G_2/M checkpoint prevents cells from entering mitosis with unreplicated or damaged DNA. In fact cell cycle analysis shows that K562 cells try to counteract the induction of apoptosis by G_2/M accumulation.

These cells are more resistant to ionizing radiation and/or etoposide, with respect to HL60 and Jurkat cells, since their blockage at G_2/M phase is more evident in all treated samples, with respect to control. Nevertheless, DNA damage is too strong for cell survival mainly upon 15 and 15 Gy plus etoposide, even though a scarce number of apoptotic cells, evidenced in these experimental conditions, is paralleled by a large amount of dead cells in 15 Gy, mainly in 15 Gy plus etoposide samples.

Since the study of the relationship between multiple survival and death pathways along with the knowledge of the molecular mechanisms of antitumor agents can be of help in

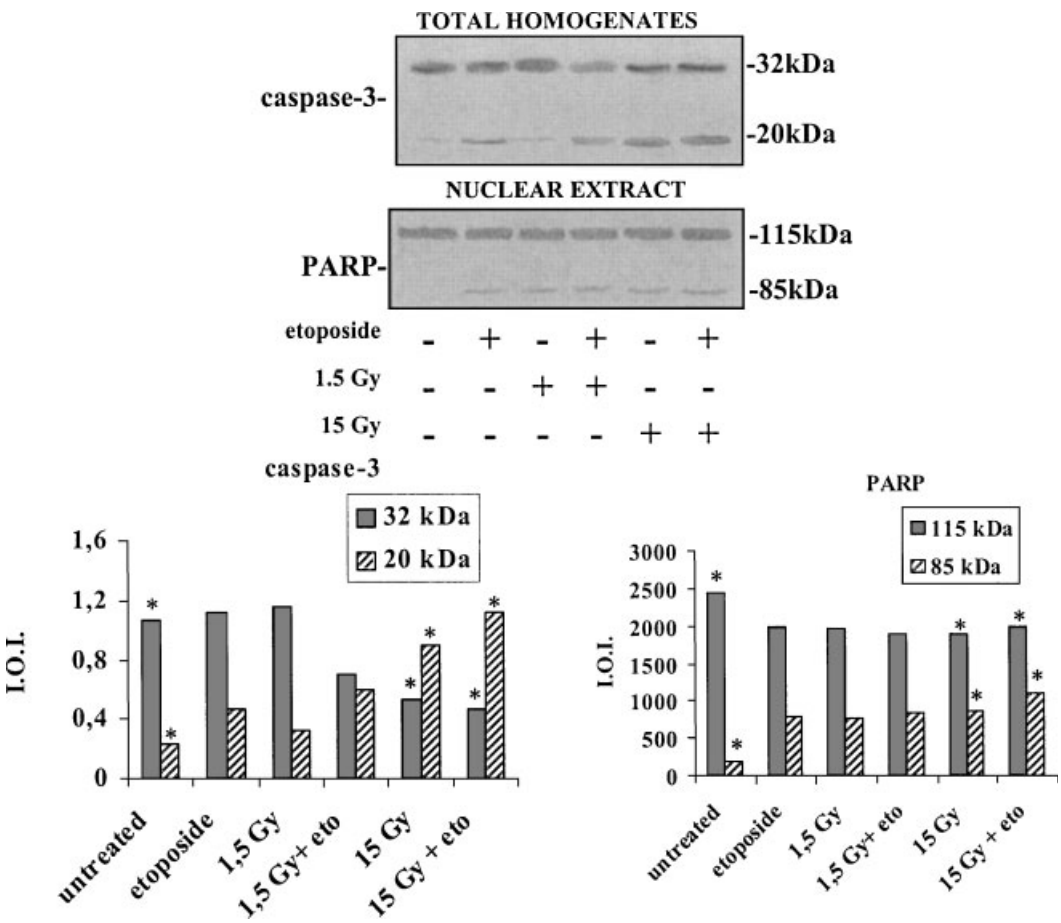

Fig. 6. Western blotting analysis of caspase-3 and PARP both (full length and fragments) in K562 cells exposed to 7 μM etoposide and/or ionizing radiation. Each electrophoretic lane has been loaded with equal amount of proteic lysate and protein levels have been quantified by densitometric analysis. Results are representative of three different experiments ± SD. Untreated versus 15 and 15 Gy plus etoposide, $P < 0.05$.

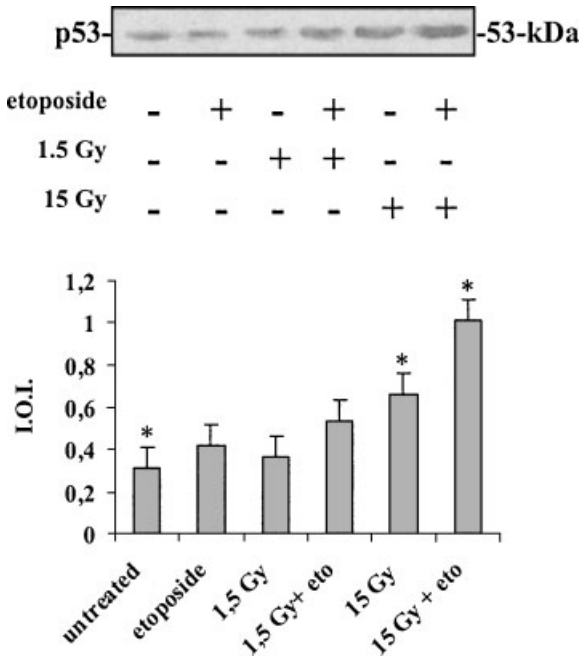

Fig. 7. Western blotting analysis of p53 expression in K562 cells exposed to 7 μM etoposide and/or ionizing radiation. Each electrophoretic lane has been loaded with equal amount of proteic lysate, and protein levels have been quantified by densitometric analysis. Results are representative of three different experiments ± SD. Untreated versus 15 and 15 Gy plus etoposide, $P < 0.05$.

setting up new therapeutical strategies against leukemia, here we examined the role of JNK/SAPK, p53, and mitochondrial pathways in the apoptotic response of K562 cell line to IR/etoposide combined treatment.

Our results let us suppose that the induction of cell death in these cells, which is evident in 15 Gy, mainly in 15 Gy plus etoposide, may be mediated by JNK/SAPK pathway, since its nuclear translocation links extracellular stimuli triggered by IR/ etoposide combined treatment to the nucleus, as elsewhere reported in other experimental models [Metzler et al., 2000]. Furthermore, JNK /SAPK pathway could be strictly linked both to p53, which discloses a significant increase of its expression, chiefly in 15 and 15 Gy plus etoposide, and to Bcl-2, which declines in the same experimental conditions. p53, paralleled by Bcl-2 decline, could allow Bax homodimerization leading to loss of membrane potential ($\Delta\psi m$), cytochrome c mitochondrial release, and caspase-9 activation, which tightly binds to Apaf-1.

Caspase-9' 37 kDa fragment production is particularly evident in samples treated with the higher radiation dose, but above all, associated with etoposide.

Active caspase-9 activates in turn cell death effector caspase-3, which cleaves PARP, as demonstrated by the presence of the 85 kDa fragment in nuclear extracts. Also in this case, the major response belongs to the two higher radiation doses. These events suggest the activation of two different pathways which join in caspase-3 activation: JNK activates p53, which, in turn, regulates death enhancing effector Bax level, and, in parallel, modulates death suppressor Bcl-2 decline.

Thus, further investigations of these and other molecular mechanisms are useful to set up new therapeutical strategies, which, overcoming resistance mechanisms, influence cell death response in human leukemic cells exposed to IR/etoposide combined treatment.

ACKNOWLEDGMENTS

Authors thank Prof. C. Ausili, Dr. Genovesi at Dipartimento di Scienze Cliniche e delle Bioimmagini, Sezione di Radioterapia Oncologica, for their skilfull assistance in setting up irradiation protocols.

REFERENCES

Alridge DR, Ratford IR. 1998. Explaining differences in sensitivity to killing by ionizing radiation between human lymphoid cell lines. Cancer Res 58:2817–2824.

Amundson SA, Myers TG, Fornace AJ. 1998. Roles for p53 in growth arrest and apoptosis: Putting on the brakes after genotoxic stress. Oncogene 17:3287–3299.

Arita D, Kambe M, Ishioka C, Kanamaru R. 1997. Induction of p53-independent apoptosis associated with G_2M arrest following DNA damage in human colon cancer cell lines. Jpn J Cancer Res 88:39–43.

Brantley-Finley C, Lyle CS, Du L, Goodwin ME, Hall T, Szwedo D, Kaushal GP, Chambers TC. 2003. The JNK, ERK, and p53 pathways play distinct roles in apoptosis mediated by the antitumor agents vinblastine, doxorubicin, and etoposide. Biochem Pharmacol 66:459–469.

Bratton SB, Cohen GM. 2001a. Apoptotic death sensor: An organelle's alter ego. Trends Pharmacol Sci 22:306–315.

Bratton SB, Walker G, Srinivasula SM, Sun XM, Butterworth M, Alnemri ES. 2001b. Recruitment, activation, and retention of caspase-9 and -3 by Apaf-1 apoptosome and associated XIAP complexes. EMBO J 20:998–1009.

Burden A, Kingma PS, Froelich-Ammon SJ, Bjornsti MA, Patchan MW, Thompson RB, Osheroff N. 1996. Topoisomerase II–etoposide interactions direct the formation of drug-induced enzyme–DNA cleavage complexes. J Biol Chem 46:29238–29244.

Cain K, Bratton SB, Cohen GM. 2002. The Apaf-1 apoptosome: A large caspase-activating complex. Biochimie 84:203–214.

Conus S, Kaufman T, Fellay I, Otter I, Rosse T, Borner C. 2000. Bcl-2 is a monomeric protein: Prevention of homodimerization by structural constraints. EMBO J 19:1534–1544.

Cookson MR, Ince PG, Usher PA, Shaw PJ. 1999. Poly ADP-ribose polymerase is found in both the nucleus and cytoplasm of human CNS neurons. Brain Res 834:182–185.

Daniak N. 2002. Hematologic consequences of exposure to ionizing radiation. Exp Hematol 30:513–528.

Davis RJ. 2000 Signal transduction by the JNK group of MAPK kinases. Cell 103:239–252.

Di Pietro R, Centurione L, Sabatini N, Bosco D, Sancilio S, Garaci F, Rana R, Cataldi A. 2004. Caspase-3 is dually regulated by apoptogenic factors mitochondrial release and by SAPK/JNK metabolic pathway in leukemic cells exposed to etoposide-ionizing radiation combined treatment. Int J Immunopathol Pharmacol 17:181–190.

Facompré M, Wattez N, Kluza J, Lansiaux A, Bailly C. 2000. Relationship between cell cycle changes and variations of the mitochondrial membrane potential induced by etoposide. Mol Cell Biol Res Comm 4:37–42.

Gajkowska B, Motyl T, Olszewska-Badarczuk H, Gniadecki R, Koronkiewicz M. 2000. Structural association of Bax with nuclear matrix and cytomatrix revealed by embedment-free immunogold electron microscopy. Cell Biol Int 24(9):649–656.

Gajkowska B, Motyl T, Olszewska-Badarczuk H, Godlewski MM. 2001. Expression of Bax in cell nucleus after experimentally induced apoptosis revealed by immunogold and embedment-free electron microscopy. Cell Biol Int 25:725–733.

Gao FC, Zhang L, Nakajiama T, Ichinose S, Hara T, Koike K, Tsuchida N. 2001. Caspase-dependent cytosolic release of cytochrome c and membrane translocation of Bax in p53-induced apoptosis. Exp Cell Res 265:145–151.

Ham J, Eliers A, Whitfield J, Neame SJ, Shah B. 2000. c-Jun and the transcriptional control of neuronal apoptosis. Biochem Pharmacol 60:1015–1021.

Hu MC, Qiu WR, Wang YP. 1997. JNK1, JNK2, and JNK3 are p53 N-terminal serine 34 kinases. Oncogene 15:2277–2287.

Kamesaki H. 1998. Mechanisms involved in chemotherapy-induced apoptosis and their implications in cancer chemotherapy. Int J Hematology 68:29–43.

Kaufmann SH, Brunet G, Talbot B, Lamarr D, Dumas C, Shafer JH, Poirier G, 1991. Association of poly ADP-ribose polymerase with the nuclear matrix: The role of intermolecular disulfide bond formation, RNA retention, and cell type. Exp Cell Res 192:524–535.

Kaufmann SH, Earnshaw WC. 2000. Induction of apoptosis by cancer chemotherapy. Exp Cell Res 256:42–49.

Kremenetskaya OS, Logacheva NP, Baryshnikov AY, Chumakov PM, Kopnin BP. 1997. Distinct effects of various p53 mutants on differentiation and viability of K562 cells. Oncol Res 9(4):155–166.

Lamarre D, Talbot B, De Murcia G, Laplante C, Leduc Y, Mazen A, Poirier GG. 1988. Structural and functional analysis of poly ADP ribose polymerase: An immunological study. Biochem Biophys Acta 950:147–160.

Law JC, Ritke MK, Yalowich JC, Leder GH, Ferrell RE. 1993. Mutational inactivation of the *p53* gene in the human erythroleukemic K562 cell line. Leukem Res 17(12):1045–1050.

Leland H, Weinert TA. 1989. Checkpoints: Controls that ensure the order of cell cycle events. Science 246:629–634.

Lowe SW, Bodis S, Bardeesy N. 1994. Apoptosis and the prognostic significance of p53 mutation. Cold Spring Harbor Symp Quant Biol 59:419–426.

Makin G. 2002. Targeting apoptosis in cancer chemotherapy. Expert Opin Ther Targets 6:73–84.

Metzler B, Hu Y, Dietrich H, Xu Q. 2000. Increased expression and activation of stress-activated protein kinases/c-jun NH(2)-terminal protein kinases in atherosclerosis lesions coincide with p53. Am J Pathol 156(6):1875–1886.

Sabatini N, Di Pietro R, Rapino M, Sancilio S, Comani S, Cataldi A. 2004. PI-3-kinase/NF-kB mediated response of Jurkat T leukemic cells to two different chemotherapeutic drugs, etoposide and TRAIL. J Cell Biochem 93:301–311.

Saleh A, Srinivasula SM, Acharya S, Fishel R, Alnemri ES. 1999. Cytochrome c and dATP-mediated oligomerization of Apaf-1 is a prerequisite for procaspase-9 activation. J Biol Chem 274:17941–17945.

Schneiderman MH, Hofer KG, Schneiderman GS. 2001. Targets for radiation induced cell death: When DNA damage doesn't kill. Radiat Res 155:529–535.

Secchiero P, Bertolaso L, Casareto L, Gibellini D, Vitale M, Bernis K, Aliotti A, Capitani S, Franchini G, Gallo RC, Zauli G. 1998. Human herpesvirus 7 infection induces profound cell cycle perturbations coupled to dysregulation of cdc2 and cyclin B and polyploidization of CD4+T cells. Blood 92:1685–1696.

Shimokawa N, Qiu CH, Seki T, Dikic I, Koibuchi N. 2004. Phosphorylation of JNK is involved in regulation of H^+-induced c-Jun expression. Cell Signal 16:723–729.

Stadheim TA, Kucera GL, 2002. c-jun N-terminal kinase/stress-activated protein kinase (JNK/SAPK) is required for mitoxantrone- and anisomycin-induced apoptosis in HL-60 cells. Leukem Res 26:55–65.

Strasser A, Harris AW, Jacks T, Cory S. 1994. DNA damage can induce apoptosis in proliferating lymphoid cells via p53-independent mechanism inhibitable by Bcl-2. Cell 79:329–339.

Verheij M, Ruiter GA, Zerp SF, van Blitterswijk WJ, Fuks Z, Haimovitz-Friedman A, Bartelink H. 1998. The role of the stress-activated protein kinase (SAPK/JNK) signaling pathway in radiation-induced apoptosis. Radiother Oncol 47(3):225–232.

Vogelstein B, Lane D, Leviere AJ. 2000. Surfing the p53 network. Nature 408:307–310.

Watters D. 1999. Moleculars mechanism of ionizing radiation induced apoptosis. Immunol Cell Biol 77:263–271.

Willaime-Morawek S, Brami-Cherrier K, Mariani J, Caboche J, Brugg B. 2003. c-Jun N-terminal kinases/c-Jun and p38 pathways cooperate in ceramide-induced neuronal apoptosis. Neuroscience 119:387–397.

Wu GS. 2004. The functional interactions between the p53 and MAPK signaling pathways. Cancer Biol Ther 3(2):156–161.

Wyllie AH, Kerr JFR, Currie AR. 1980. Cell death: The significance of apoptosis. Int Rev Cytol 68:251–306.

Zauli G, Vitale M, Falcieri E, Gibellini D, Bassini A, Celeghini C, Columbaro M, Capitani S. 1997. In vitro senescence and apoptotic cell death of human megakaryocytes. Blood 90:2234–2243.